HPV16-associated tumors control myeloid cell homeostasis in lymphoid organs, generating a suppressor environment for T cells

Simone Cardozo Stone,* Renata Ariza Marques Rossetti,* Aline Bolpetti,[†] Enrique Boccardo,[‡] Patricia Savio de Araujo Souza,[§] and Ana Paula Lepique*,[1]

*Departments of Immunology and [‡]Microbiology, Institute of Biomedical Sciences, University of São Paulo, Brazil; [†]Department of Pathology, Medical School, São Paulo State University, Brazil; and [§]Department of Immunobiology, Federal Fluminense University and Program of Cellular Biology, Brazilian National Cancer Institute, Rio de Janeiro, Brazil

ABSTRACT

Tumors are complex structures containing different types of cells and molecules. The importance of the tumor microenvironment in tumor progression, growth, and maintenance is well-established. However, tumor effects are not restricted to the tumor microenvironment. Molecules secreted by, as well as cells that migrate from tumors, may circulate and reach other tissues. This may cause a series of systemic effects, including modulation of immune responses, and in some cases, leukocytosis and metastasis promotion. Leukocytosis has been described as a poor prognostic factor in patients with cervical cancer. The main etiological factor for cervical cancer development is persistent infection with high oncogenic risk HPV. Our laboratory has been exploring the effects of high oncogenic risk, HPV-associated tumors on lymphoid organs of the host. In the present study, we observed an increase in myeloid cell proliferation and alteration in cell signaling in APCs in the spleen of tumor-bearing mice. In parallel, we characterized the cytokines secreted in the inflammatory and tumor cell compartments in the tumor microenvironment and in the spleen of tumor-bearing mice. We show evidence of constitutive activation of the IL-6/STAT3 signaling pathway in the tumor, including TAMs, and in APCs in the spleen. We also observed that IL-10 is a central molecule in the tolerance toward tumor antigens through control of NF-κB activation, costimulatory molecule expression, and T cell proliferation. These systemic effects over myeloid cells are robust and likely an important problem to be addressed when considering strategies to improve anti-tumor T cell responses. *J. Leukoc. Biol.* **96: 619–631; 2014.**

Introduction

Solid tumors are complex tissues that contain tumor cells, endothelial cells, pericytes, inflammatory cells, fibroblasts, and also acellular components, such as cytokines, inflammatory mediators, and extracellular matrix. Within the tumor microenvironment, the different elements are able to induce angiogenesis, inactivate anti-tumor T cell responses through various mechanisms, and promote tumor cell survival and proliferation [1]. Tumor-infiltrating inflammatory cells may have a dual effect. Whereas these cells are an important line of defense against tumor onset—generating reactive oxygen species, secreting proinflammatory cytokines, and causing cytotoxicity—they may also act as promoters of cell transformation, playing an important role in tumor progression [2, 3]. Besides, cells with anti-inflammatory and suppressor properties, such as MDSCs, M2, and regulatory macrophages and T_{regs} are commonly found in established tumors. These cells can dampen anti-tumor T cell responses, facilitating tumor growth [4–6]. The presence of an inflammatory infiltrate implies that tumors secrete factors capable of recruiting these cells. Of note, it has been reported that tumors secrete factors that induce cell proliferation in lymphoid tissues [7], which includes myeloid cells with immature phenotype and suppressor characteristics [8]. Moreover, 1 g of tumor tissue contains 10^8–10^9 cells [9]; if 5%

The online version of this paper, found at www.jleukbio.org, includes supplemental information.

1. Correspondence: Dept. of Immunology, ICB/USP, Av. Prof. Lineu Prestes, 1730, Room 136, São Paulo, SP, Brazil. E-mail: alepique@icb.usp.br

of these correspond to inflammatory cells, a tumor would have 5×10^6–10^7 inflammatory cells/g of tissue. Therefore, the identification of the role and source of these cells is important for understanding tumor biology. Importantly, these cell populations constitute a target for interference that may contribute to destabilizing tumor growth and progression.

HPV are small DNA viruses that infect epithelial cells of skin and mucosa. Infection with high oncogenic risk HPV types is the main etiological factor for cervical cancer, where virtually all tumors harbor HPV DNA [10]. HPV is also the etiological factor of a significant percentage of anogenital and oropharyngeal tumors [11, 12]. Data from several studies demonstrated that HPV-associated cervical lesions are infiltrated by macrophages and lymphocytes [13–17]. In fact, the ratio between CD8 T cells and T_{regs} in primary tumors is a prognostic marker for cervical cancer [17]. Besides the tumor microenvironment, HPV-specific, circulating CD4 T cells, with effector and/or regulatory phenotype, are present in the peripheral blood of patients. The phenotype of lymphocytes depends on the cervical lesion progression. Asymptomatic women preferentially display Th1-effect responses, whereas women with cancer also display T_{regs} [18]. Cervical tumors may also influence other leukocyte populations. Patients with recurrent cervical cancer and leukocytosis live for significantly shorter periods, free of disease, than women with recurrent cancer but normal circulating leukocyte numbers [19].

Our laboratory has used the mouse HPV16 tumor model, TC-1 [20], to study interactions between tumor cells and the host immune system, not only restricted to the tumor microenvironment but also in lymphoid organs [21]. We have shown previously that TC-1 tumor-bearing mice exhibited a significant increase in myeloid populations in the spleen, as well as B lymphocytes in peripheral lymph nodes [21, 22]. We have also shown, using cervical cancer-derived cell lines grafted in immunodeficient mice, that proliferation and accumulation of myeloid cells in lymphoid organs are HPV-mediated effects [23]. TC-1 tumors recruit M2-like macrophages (TAMs), which are capable of suppressing anti-tumor T cell responses. We also showed that this effect is partially dependent on IL-10 expression by TAM [21, 22]. In this model, TAM corresponds to ~10% of the total number of tumor cells. Therefore, modulation of TAM could be an important anti-tumor therapeutic tool. To accomplish this goal, we must have a more complete understanding of the local and systemic effects of the tumor on TAM and other myeloid cell populations that orchestrate immune responses in the host.

In this manuscript, we characterized cytokine expression and signaling pathways in the tumor microenvironment in the inflammatory and tumor cell compartments, as well as in lymphoid organs. Our data show that tumor-bearing mice exhibited an accumulation of myeloid cells with a suppressive phenotype: low expression of IL-12 and costimulatory molecules. The phenotype, but not the number of these cells, was modulated by IL-10, possibly through NF-κB inhibition. At the same time, STAT3 and Akt were constitutively activated, which could promote myeloid cell proliferation and accumulation. We believe that our data will contribute to the design of new protocols to modulate the phenotype of TAM or APC in the host.

MATERIALS AND METHODS

Specifications about antibodies used in the work are listed in Supplemental Material 1.

Cell lines

TC-1 tumor cells are transformed with Ej-ras and HPV16 E6 and E7 oncogenes [20] and were kindly donated by Dr. T-C. Wu (Johns Hopkins University, Baltimore, MD, USA). SiHa, a HPV16 cervical cancer-derived cell line [24], was purchased from the American Type Culture Collection (Manassas, VA, USA).

Mouse tumor model and assessment of in vivo cell proliferation

TC-1 cells were s.c.-injected in the dorsal flank of C57BL/6 mice, RAG1$^{-/-}$ mice (B6.129S7-Rag1^{tm1Mom}/J; The Jackson Laboratory, Bar Harbor, ME, USA), or IL-10$^{-/-}$ mice (B6.129P2-IL10^{tm1Cgn}; The Jackson Laboratory); 10^5 cells suspended in 100 μl 1 mM CaCl$_2$, 0.5 mM MgCl$_2$-supplemented PBS generated detectable tumors within 7–10 days postinjection. Mice were killed 24 days later or when tumors reached 8 mm in the largest diameter.

C57BL/6 mice were bred and maintained in specific, pathogen-free conditions in the Isogenic Mouse Facility at the Department of Immunology, ICB/USP (Brazil). All our procedures involving mice were in accordance with the guidelines of the Animal Care Committee, ICB/USP, and approved under Protocol Number 2011/151.

For proliferation assays, we injected naive or tumor-bearing mice with 1 mg BrdU (BrdU detection kit; BD Biosciences, San Jose, CA, USA), diluted in PBS solution, 1 h before death.

Cell suspension preparations

All cell preparations were made using ice-cold 1× Hanks' solution with 15 mM HEPES, pH 7.4, 0.5 U/mL DNase I (Worthington Biochemical, Lakewood, NJ, USA) and 5% FBS. Spleen suspensions were obtained by tissue dissociation through a 70-μm metal mesh and red cell lyses in hypotonic buffer. Bone marrow was harvested from tibias, femurs, and iliac crests by flushing with the buffer described above. Red cells were eliminated by hypotonic lyses. Lymph node cell suspensions were obtained by mechanical dissociation. Tumor cell suspensions were obtained by digestion of finely minced tissue with 1 mg/mL Collagenase I and IV (Worthington Biochemical) in a Thermomixer (Eppendorf, Germany) at 37°C for ~1 h. Cell viability, accessed by Trypan blue staining, in the final suspensions was between 90% and 95%.

Flow cytometry analysis

All cells were incubated in the same buffer described for cell suspension preparations. FcBlock (BD Biosciences) was added to cells before specific antibodies and incubated for 15 min. Cells were stained with specific antibodies against cell surface markers, as indicated in each figure (listed in Supplemental Material 1). When necessary, following surface staining, cells were fixed and permeabilized with 90% methanol for following incubation with antibodies against signaling proteins [25] or fixed for DNAse I digestion before incubation with anti-BrdU antibody. BrdU detection protocol was performed according to instructions in the BrdU Detection Kit (BD Biosciences). Antibodies against total and phosphorylated proteins involved in signal transduction, Akt, NF-κB, IκB, STAT3, STAT5, JAK2, Erk, and CREB were purchased from Cell Signaling Technology (Beverly, MA, USA; Supplemental Material 1). Flow cytometry was performed in a FACSCalibur or FACSCanto II (BD Biosciences), where 30,000–50,000 events were acquired. Data obtained were analyzed with FlowJo software (TreeStar, Ashland, OR, USA).

Cell sorting

Total tumor cell suspensions were sorted in CD45$^-$ and CD45$^+$ (tumor cells, endothelial cells, pericytes, fibroblasts, and inflammatory infiltrate,

respectively), using CD45$^+$ magnetic beads and LS+ columns attached to magnets (Miltenyi Biotec, Germany). Alternatively, total tumor suspensions were sorted in CD45$^-$, CD45$^+$CD11b$^+$F4/80$^+$ cells (macrophages) and CD45$^+$CD11b$^+$Gr1$^+$ (granulocytes or possibly, MDSCs). These cell separations were performed using a FACSAria II (BD Biosciences), after blocking and cell labeling with the indicated antibodies (Supplemental Material 1). All FACS-sorted populations were gated in a DAPI$^-$ window to enrich for live cells. Spleen total nucleated cell suspensions were sorted in MHC-II$^+$ and MHC-II$^-$ cells, using MHC-II$^+$ magnetic beads and LS+ columns attached to magnets (Miltenyi Biotec). All sorted populations were, at least, 98% pure.

T cell suppression assay

Lymph node suspensions from naive C57BL/6 mice were labeled with Cell-Trace Violet (Life Technologies, Carlsbad, CA, USA), as indicated by the manufacturer. Labeled cells were seeded in round-bottom wells and incubated with PHA (Life Technologies), diluted 1:100 in 10% FBS RPMI (PHA concentration was previously titrated from a stock solution). In part of the wells, CD11b$^+$-sorted cells from spleens of tumor-bearing mice were added to the culture in a 1:5 (myeloid:lymphocyte) ratio. Five days later, cells were harvested, incubated with antibodies against CD4 and CD8, and analyzed by flow cytometry.

Western blotting

Sorted CD45$^+$ and CD45$^-$ from TC-1 tumors and HeLa cells as controls were lysed in radioimmunoprecipitation assay buffer (20 mM Tris-HCl, pH 7.5, 150 mM NaCl, 1 mM Na$_2$ EDTA, 1 mM EGTA, 1% Nonidet P-40, 1% sodium deoxycholate), containing protease inhibitor cocktail for mammalian cells and tissue extracts and phosphatase inhibitor cocktail (P8340 and P0044, respectively; Sigma-Aldrich, St. Louis, MO, USA). Cell lysates were quantified using the bicinchoninic acid Protein Assay kit (Thermo Scientific, Rockford, IL, USA). Each cell lysate (50 μg) was fractionated in 8% or 12% SDS-PAGE. Proteins were transferred to PVDF membranes and probed with Cell Signaling Technology antibodies mentioned above, followed by incubation with HRP-conjugated anti-rabbit antibody, which was detected using chemiluminescent reaction (ECL Kit; GE Healthcare, Little Chalfont, UK) to impress X-ray films.

Immunofluorescence

TC-1 tumor fragments or spleen from naive and tumor-bearing mice were frozen in Tissue-Tek O.C.T. (Sakura Finetek, The Netherlands) immediately after harvesting; 5 μm cryo-sections were mounted on pretreated glass slides and fixed in a methanol/acetone solution (1:2) at room temperature for 5 min. Sections were air-dried and rehydrated in three incubations in PBS. Only tumor sections were blocked with FcBlock and incubated with anti-CD11b conjugated to biotin (BD Biosciences). After washing, sections were incubated with Alexa-594-conjugated streptavidin (Life Technologies). After washing with PBS, stained tumor section and unstained spleen sections were fixed with a buffered 4% formaldehyde solution, washed, and incubated with 1.5 M HCl for 15 min for DNA denaturation and neutralized with 0.1 M Na$_2$B$_4$O$_7$ solution, pH 8.5, for 10 min. After washing, sections were incubated with FITC-conjugated anti-BrdU (BD Biosciences), washed, and mounted with Vectashield mounting medium for fluorescence with DAPI (Vector Laboratories, Burlingame, CA, USA). Images were obtained with an Olympus BX61, with attached DP70 Olympus camera and its own software (Olympus, Japan).

Determination of cytokine-expression profile—mRNA analyses

For RNA expression analysis, we used the Mouse Inflammatory Cytokines and Receptors RT^2 Profiler PCR Array System (PAMM-011A; SABiosciences, Qiagen, Hilden, Germany). Real-time PCR arrays were performed on an ABI Prism 7300 sequence detection system (Applied Biosystems, Foster City, CA, USA), using SYBR Green Master Mix (Applied Biosystems, Cheshire, UK). The

mRNA expression levels were represented by the ΔCt/control Ct relative values, which were calculated as the subtraction of the Ct averages of the HKG from the Ct averages of the TG [(ΔCt=CtTG−CtHKG)/CtHKG]. The amplification efficiencies of the targets (TG) and references (HKG) displayed no significant differences (data provided by SABiosciences, Qiagen). We defined that all relative expression values above the average of expression of all targets in the platform were positive; in our experiments, these threshold values were 0.3202 for CD45$^+$ cDNA and 0.3206 for CD45$^-$ cDNA. We also indicated, in the correspondent figures, the relative value 0.2, which distinguishes cDNA from genes with expression closer to HKGs.

Determination of cytokine-expression profile—protein analyses

To determine the cytokine and chemokine expression levels, we used the Mouse Cytokine Array Panel (Cat. Number ARY006; Proteome Profiler Array; R&D Systems, Minneapolis, MN, USA). Protein extracts from TC-1 tumor-sorted populations and pM were prepared, as specified by the kit protocol. The assays were performed according to the manufacturer's instructions. After the chemiluminescent reaction (ECL Kit; GE Healthcare) for detection of the bound cytokines, the membranes were exposed to X-ray films for various periods of time to guarantee signals in the linear range for densitometry. Scanned autoradiogram images were analyzed and quantified with ImageJ software (U.S. National Institutes of Health, Bethesda, MD, USA). For these experiments, as a result of lack of housekeeping targets, as in the RNA expression platform, we decided to use a reference populations. We chose pM as the reference population, as they come from the same strain of mice that we used for tumor growth and as these cells should not be activated in naive mice in our mouse facility. Therefore, these cells should display low, basal levels of cytokines and chemokines. We represented the results obtained from these experiments as relative values, where the average correspondent to six spots of background signal was subtracted from the absolute values of each cytokine. This was performed with all cytokines from all populations evaluated. From these values, we calculated the ratio between CD45$^-$ or TAM or CD11b$^+$Gr1$^+$ cells against naive pM. We also used the Mouse Cytokine Array Panel to study cytokine expression in the spleen of naive and tumor-bearing mice and the Mouse Phospho-Receptor Tyrosine Kinase Array (Proteome Profiler Array; R&D Systems) to study activation of tyrosine kinase receptors in the bone marrow of tumor-bearing and naive mice. Data obtained from these experiments were represented as a ratio between expression of a target protein between tumor-bearing and naive samples, where Value 1 indicates that this molecule is expressed at the same levels in tissues from both experimental groups. For bone marrow studies, we mechanically dissociated bone marrow cells and lysed according to the kit manufacturer's instructions.

C57BL/6 and RAG1$^{-/-}$ chimeras

A total of 2 × 10^6 T cells isolated from naive C57BL/6 mice was transplanted through tail-vein injection into RAG1$^{-/-}$ recipients, previously injected or not with 10^5 TC-1 cells. At the moment of T cell transplant, recipients displayed tumor volumes of 50–100 mm^3 (~0.5-cm diameter). Fourteen days after T cell transplant, we harvested lymph nodes of transplanted mice, prepared single-cell suspensions, and stained cells with antibodies against CD4 and CD25. We immediately fixed and permeabilized cells with the Cytofix/Cytoperm kit (BD Biosciences) and stained with anti-Foxp3 (eBioscience, San Diego, CA, USA). We used a BD FACSCalibur to analyze cells.

Statistical analysis

We used the *t*-test and ANOVA one-way to compare data obtained from naive and tumor-bearing groups, considering the differences between groups significant when $P < 0.05$.

RESULTS

TC-1 tumors promote myeloid cell proliferation in the tumor microenvironment and spleen

According to data from our laboratory and others, HPV16-associated tumors promote accumulation of myeloid cells in the spleen of tumor-bearing mice [21, 23, 26]. Leukocytes may accumulate in tissues as a result of increased recruitment, increased proliferation, reduction of cell death, or a combination of any of these factors. To test whether TC-1 tumor cells can promote myeloid cell proliferation, we injected an analog of thymidine, BrdU, in naive and tumor-bearing mice to determine the percentage of proliferating cells in different leukocyte populations. First, we observed that macrophages in the tumor microenvironment incorporated BrdU (**Fig. 1A**). It is possible that these cells were recruited to the tumor microenvironment, while already committed to progress through the cell cycle, or signals generated in the tumor could trigger proliferation within the tumor microenvironment. In the spleen, we observed a significant increase in BrdU incorporation compared with naive mice (Fig. 1B and C). Importantly, our data showed that regions of the spleen with higher BrdU incorporation corresponded to red pulp areas, suggesting that the observed cell proliferation was not related to triggering of adaptive immune responses (i.e., proliferation of antigen-activated B or T lymphocytes). Indeed, with the analysis of specific populations, it became clear that CD11bGr1low myeloid cells and macrophages displayed a significant increase in BrdU incorporation compared with the same populations in naive mice (1.8- and 4.9-fold, respectively). Interestingly, we did not observe

significant differences in cell proliferation in the bone marrow or lymph nodes of tumor-bearing mice compared with naive mice (data not shown). On the other hand and as published previously and shown below, there was an increase in the number of B lymphocytes [22] and myeloid cells in these tissues (Fig. 1D). CD11b$^+$Gr1^{low} cells may represent an immature myeloid population or even MDSC [27]. At this point, we could speculate that CD11b$^+$Gr1^{low} cells migrate to the tumor and differentiate in the predominant macrophage population. However, we have not done the experiments to test this hypothesis.

Although we did not observe a significant increase in BrdU incorporation in the bone marrow, there was an increase in the myeloid cell percentage in this tissue, indicating that tumors had an effect on this tissue. Tyrosine kinase receptors respond to several factors secreted locally or systemically. Factors secreted by tumors could signal in the bone marrow promoting cell accumulation, for example, as a result of increased survival. Indeed, with the use of an antibody array platform, we observed that there was significantly higher expression of phosphorylated tyrosine kinase receptors in the bone marrow of tumor-bearing mice than in the cell from naive mice. For instance, phosphorylated Axl, Dtk, Tie-2, EphA7, and EphB1 protein levels had an increase of 3.4-fold, 8.2-fold, 12-fold, 10-fold, and 10.2-fold, respectively, in tumor-bearing mice. The EphB4-phosphorylated form was the only receptor down-regulated in tumor-bearing mice compared with naive mice (the complete set of results is shown in Supplemental Material 2).
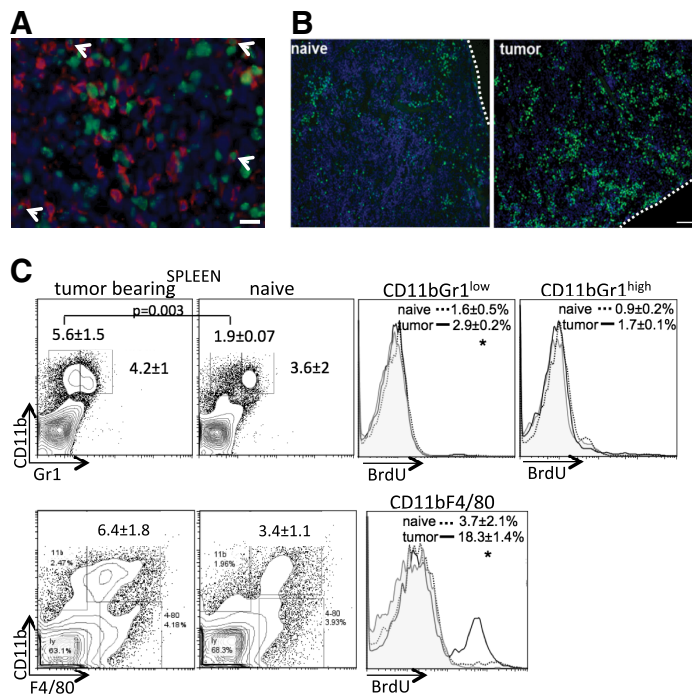

Figure 1. Myeloid cell proliferation and accumulation in TC-1 tumor-bearing mice. (A and B) Immunofluorescence analysis of tumor (A) and spleen (B) of tumor-bearing and naive mice injected with 1 mg BrdU, 1 h before euthanasia. Cryo-sections of harvested tissues were incubated with anti-CD11b-Alexa 549 (A; red staining) antibody, followed by fixation and treatment to expose incorporated BrdU and incubation with FITC-conjugated anti-BrdU (green staining). Slides were mounted with Vectashield with DAPI (blue staining). Images were acquired with a BX61 Olympus microscope. (A) 1000× magnification; bar indicates 10 μm; arrowheads indicate CD11b$^+$ (red cells) incorporating BrdU (green nuclei). (B) 100× magnification; bar indicates 10 μm. Spleens from tumor-bearing and naive mice are indicated. (C and D) Detection of myeloid populations and BrdU incorporation in the spleen and bone marrow, respectively. Dot plots correspond to flow cytometry analyses of single-cell suspensions stained with antibodies against the indicated markers. Percentages of specific populations are indicated in the graphs. Histograms correspond to BrdU incorporation within each indicated population. *Significant differences in BrdU incorporation between naive and tumor-bearing mice in a given population ($P < 0.05$). Each experimental group contained four animals. Macrophage populations in the bone marrow were similar between naive and tumor-bearing mice (data not shown).

TC-1 tumors express cytokines for cell recruitment, myeloid cell proliferation, and phenotype modulation

The results described above indicated that the TC-1 tumor displayed systemic effects, which could be accomplished by secretion of soluble molecules. Cytokines play a key role in immune response control and immune system homeostasis. They can also have a role in tumor progression, angiogenesis, and immune evasion. For example, IL-1β is known to promote chronic inflammation, favoring cell transformation and tumor progression [28], whereas IL-6 may induce tumor cell proliferation and modulation of the inflammatory tumor infiltrate [29], and TGF-β promotes tolerance toward tumor antigens [30]. To identify cytokines that could affect myeloid cells locally and systemically in tumor-bearing mice, we performed mRNA and protein-expression profile analysis in ex vivo-sorted tumor cells (CD45$^-$ population) and in the inflammatory infiltrate (TAMs with phenotype CD45$^+$CD11b$^+$F4/80$^+$ and CD11b$^+$Gr1$^+$ myeloid cells; also, CD45$^+$ leukocytes from SiHa, HPV16-positive tumors grown in RAG1$^{-/-}$ mice). In **Fig. 2**, we show results of protein-expression profiles in the different tumor cell populations. Overall, the features that should be highlighted are: (1) in spite of a different immune status of the host mouse lineages, TAM from TC-1 and leukocytes from SiHa tumors display remarkably similar cytokine-expression profiles; (2) all tumor cell populations express at least one chemokine with a known role in recruitment of myeloid cells, as CCL2; (3) only CD45$^-$ tumor cells expressed growth factors for leukocytes; (4) among infiltrating leukocyte populations in TC-1 tumors, there was a mix of proinflammatory and suppressor cytokine expression, as IL-1β and IL-10; (5) we detected C5a in all tumor cell populations; (6) CD11b$^+$Gr1$^+$ myeloid cells expressed a subset of cytokines different than TAM in TC-1 tumors, indicating that these populations not only display different cell-surface markers but also should play different roles in the tumor microenvironment. Interestingly, our RNA expression data showed that CD45$^+$-infiltrating cells in TC-1 tumors expressed receptors for some of the chemokines expressed by TC-1 cells and by TAMs (Supplemental Material 3), for example, CCR2 to CCL2 and CCR3 to CCL3, indicating that there may be a positive loop where recruited cells expressed chemokines to recruit even more cells to the tumor.

Regarding the CD11b$^+$Gr1$^+$ population in the tumor, functional assays are needed to determine whether this is a granulocyte population, as neutrophils or possibly MDSCs. The cytokine-expression profile of these cells suggests that they may have a proinflammatory phenotype: positive expression of IL-1β and TREM-1 and negative expression of IL-10.

Of note, we found IL-6 expression in TC-1 tumor cells. We also observed that TAM and CD45$^+$ cells from SiHa tumors expressed IL-5 and IL-10. Interestingly, we observed that leukocytes infiltrating TC-1 tumors expressed the mRNAs for IL-10R and IL-6R (Supplemental Material 3), indicating the existence of paracrine signaling within the tumor, as expected.

Proliferation and survival signals are constitutive in the tumor microenvironment

All factors described above are chronically expressed in the tumor microenvironment. Therefore, it is reasonable to as-

sume that signaling pathways triggered by their receptors may be regulated. To test this hypothesis, we decided to screen the status of activation of signaling pathways related to cell proliferation, survival, and inflammatory responses in tumor and inflammatory cells. For this purpose, we used antibodies to detect phosphorylated and total proteins from key signaling pathways: Akt, Erk, STAT3, CREB, and NF-κB. We chose antibodies that recognize phosphorylation sites associated with protein activation (Supplemental Material 1). We sorted tumor and inflammatory cells to study the expression of these proteins. As can be observed in **Fig. 3A**, STAT3, Akt, Erk, and CREB were expressed in both cell populations in their total and phosphorylated forms. As the anti-phospho-CREB antibody also recognizes ATF1, our results show that ATF1 was phosphorylated mainly in the TC-1 tumor cells (Fig. 3A). Importantly, although we loaded equal amounts (50 μg) of protein from all cell lysates, the concentration of these proteins seemed always reduced in the inflammatory cells compared with tumor cells, indicating higher expression of these proteins in the tumor cells. The control lysates from the HeLa cell line were loaded in smaller amounts—25 μg proteins—as a result of the strong signal they generated in this type of experiment. Interestingly, HeLa cells, which are transformed with HPV18—another high-oncogenic risk HPV type—displayed high basal levels of phosphorylated proteins, some of them up-regulated by treatment with 10 ng PMA for 30 min.

As we were not able to detect the RelA (p65) component of NF-κB by Western blotting, we used intracellular staining and flow cytometry to evaluate this pathway. NF-κB serine 536 was not phosphorylated in TAM (Fig. 3B), indicating that NF-κB was less active in these cells. We used Akt as a control for this type of staining and observed consistent results with those obtained by Western blottings.

Tumors control cytokine expression and signaling pathways in the spleen

Considering that many of the factors expressed in the tumor microenvironment were soluble proteins that could mediate systemic effects and that there was an increase in cellularity in the spleen of tumor-bearing mice, we decided to investigate the status of signaling pathways and the cytokine-expression profile in the spleen of tumor-bearing mice. As expected, we found a significant increase in myeloid cells in the spleen of tumor-bearing mice (**Fig. 4A**) and focused our observations in the myeloid APCs (CD19$^-$MHC-II$^+$). The rationale for this choice was that these cells have an essential role in determining T cell responses, controlling, therefore, the tumor fate. Moreover, we have shown accumulation of myeloid cells in the host. Therefore, we wished to determine myeloid APC function. As shown in Fig. 4B, several pathways were differentially activated in this population in naive and tumor-bearing mice. We observed significantly lower expression levels of IκB-, NF-κB-, and ERK-phosphorylated proteins in cells from tumor-bearing mice than in cells from naive animals. On the other hand, JAK2-, STAT3-, and STAT5-phosphorylated forms were up-regulated in cells from these animals compared with naive mice. Akt expression, measured by MFI, was the same in populations from both experimental groups, although the expres-
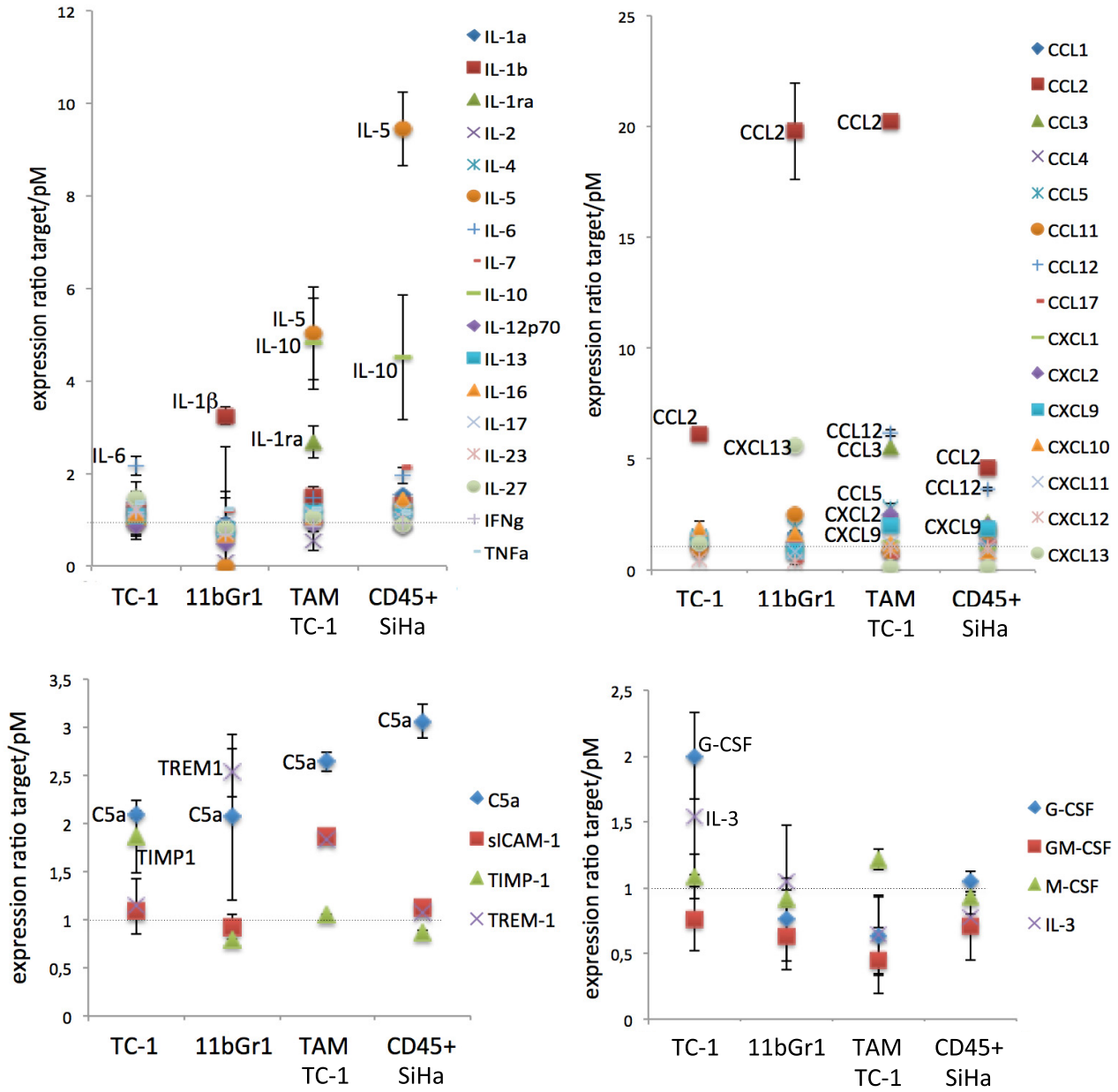
Figure 2. Protein-expression profile of CD45⁻ tumor cells, TAMs, and CD11b⁺Gr1⁺ tumor-infiltrating cell populations. Lysates (50 μg) from the indicated sorted populations were incubated with membranes from the Cytokine Proteomic Array (R&D Systems). The expression of each cytokine was compared with the expression of the same cytokine in a lysate of pM mice. Graph abciss shows cells that originated the lysates for these experiments. TC-1 (sorted CD45- cells from TC-1 tumors; 11bGr1, sorted CD11b+Gr1+ from TC-1 tumors; TAM TC-1, sorted TAM from TC-1 tumors; CD45+ SiHa, sorted CD45+ cells from SiHa tumors). Relative results correspond to the average of three independent experiments, where we subtracted the background absolute densitometry value from each cytokine absolute signal and then calculated the ratio between a given cytokine in the target populations and pM. Names of molecules within the graph area indicate those in which expression was significantly different than the expression in pM. The line indicates the Value 1, where cytokine expression is the same in the target population and pM. The values presented correspond to three independent experiments.

sion pattern was different between them. Interestingly, STAT5 displayed the same expression pattern: two peaks in naive mice that condensed in one peak of intermediate intensity in tumor-bearing mice, indicating constitutive, even if intermediate, activity. However, in the case of STAT5, the average MFI

was significantly higher in tumor-bearing mice. CREB-, STAT1-, and JNK-phosphorylated proteins did not show significant differences between naive and tumor-bearing mice.

As various signaling pathways, altered in the spleen of tumor-bearing mice, control cytokine expression, we sought to
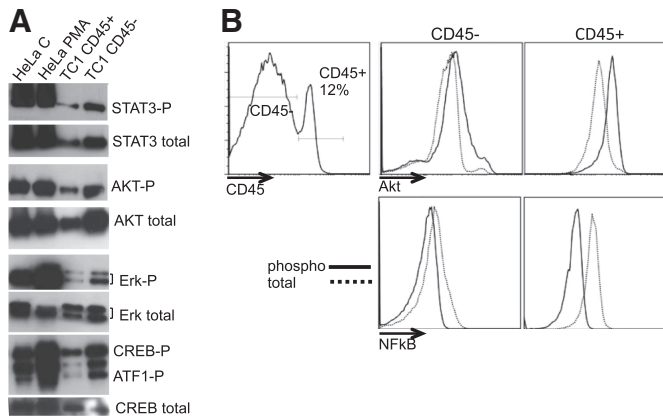
Figure 3. Signaling pathways in the tumor microenvironment. Detection of total and phosphorylated proteins involved in signal transduction by Western blotting (A) and flow cytometry (B). (A) Tumor cell lysates (50 μg; TC1 CD45$^-$ and TC1 CD45$^+$), 25 μg untreated HeLa cells (HeLa C), and 30 min, 10 ng/ml PMA-treated HeLa cells (HeLa PMA) cell lysates were fractioned in SDS-PAGE, transferred to PVDF membrane, and probed with the indicated antibodies. (B) Tumor cell suspensions were stained with anti-CD45, fixed, permeabilized, incubated with anti-Akt or NF-κB (p65) antibodies, as indicated, and analyzed by flow cytometry. Histogram to the left corresponds to the CD45$^-$ and CD45$^+$ population percentages within the tumor as indicated; other histograms show phosphorylated and total protein expression (Akt above, NF-κB below) gated on the CD45$^-$ and CD45$^+$ populations as indicated.

determine the cytokine expression pattern in total splenocytes and MHC-II$^+$ APCs in the spleen. In **Fig. 5A**, we show a cytokine-expression ratio in the populations mentioned above in tumor-bearing and naive mice. We could readily observe that there were more down-regulated than up-regulated cytokines in the spleens of tumor-bearing mice (cytokines bellow the black line, Ratio Value 1). A second general observation was that the expression pattern between total and MHC-II$^+$ cells in the spleen was somewhat similar, suggesting that most differences in cytokine expression were a result of modulation of cytokine expression in APCs. A third interesting observation was that cytokines, such as IL-6 and IL-10, which may play a role in cell signaling in the spleen (through activation of JAK2/STAT3), were not expressed in this tissue, suggesting that their source was the tumor or other tissues. On the other hand, CCL2 was highly expressed in the spleens of tumor-bearing mice, as well as other chemokines that recruit myeloid cells, such as CCL1, CCL2, and CXCL1. However, cytokines involved in the recruitment of activated T cells, as CXCL9 and CXCL10, were down-regulated in the spleens of tumor-bearing mice. Interestingly, similar to the CD11b$^+$Gr1$^+$ population in the tumor, we observed positive expression of TREM-1 in total nucleated spleen cells and MHC-II$^+$ cells. Although we observed a significant increase in IL-1β expression in the spleen of tumor-bearing mice compared with naive mice, we also observed expression of the IL-1ra molecule, which inhibits IL-1 signaling [31]. TNF-α was down-regulated in the total spleen preparations, whereas IL-12p70 was down-regulated in professional APCs (MHC-II$^+$). These findings corre-

lated with the inactivation of the NF-κB pathway [32]. We found increased expression of IL-5 and IL-17 in the spleens of tumor-bearing mice but not in APCs, indicating that their expression could be restricted to T cells in this tissue. As we had previously detected IL-5 expression in TAM, we decided to investigate whether IL-5 had an effect on tumor growth and the quality and frequency of tumor-inflammatory infiltrate and systemic leukocyte populations' homeostasis. The treatment of TC-1 tumor-bearing with anti-IL-5-neutralizing antibody caused no significant differences in any of these parameters, indicating that IL-5 had no obvious effect on anti- or protumoral immune responses (data not shown). We also observed down-regulation of IL-4 and IL-13—cytokines that are hallmarks of Th2 responses—in the spleen of tumor-bearing mice (Fig. 5A).
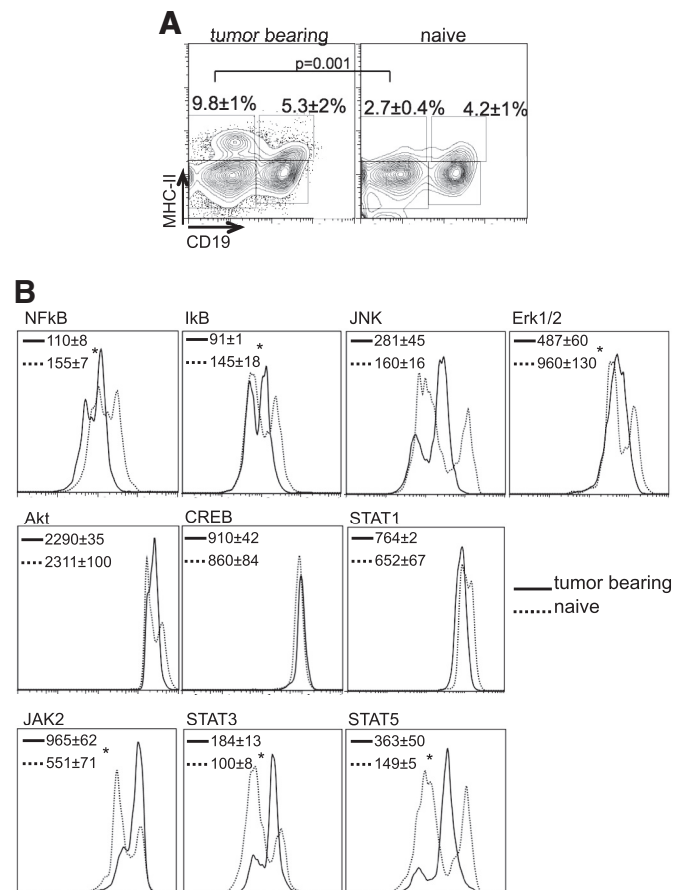

Figure 4. Analysis of Akt and NF-κB signaling pathways in the spleen of tumor-bearing mice. Nucleated spleen-cell suspensions were stained with antibodies against the indicated surface markers, fixed, permeabilized, stained with antibodies against the indicated phosphorylated proteins, and analyzed by flow cytometry. (A) Antigen-presenting cell frequencies in tumor-bearing and naive mice, according to CD19 and MHC-II expression. (B) All histograms corresponded to the CD19$^-$MHC-II$^+$ population, where we compared protein expression in the indicated populations of naive (dotted lines) and tumor-bearing (solid lines) mice. Values in the dot plots correspond to the average MFI of each protein. We used three mice/group. At least 10,000 events of the rarest population were acquired. *Significant differences between experimental groups ($P<0.05$).
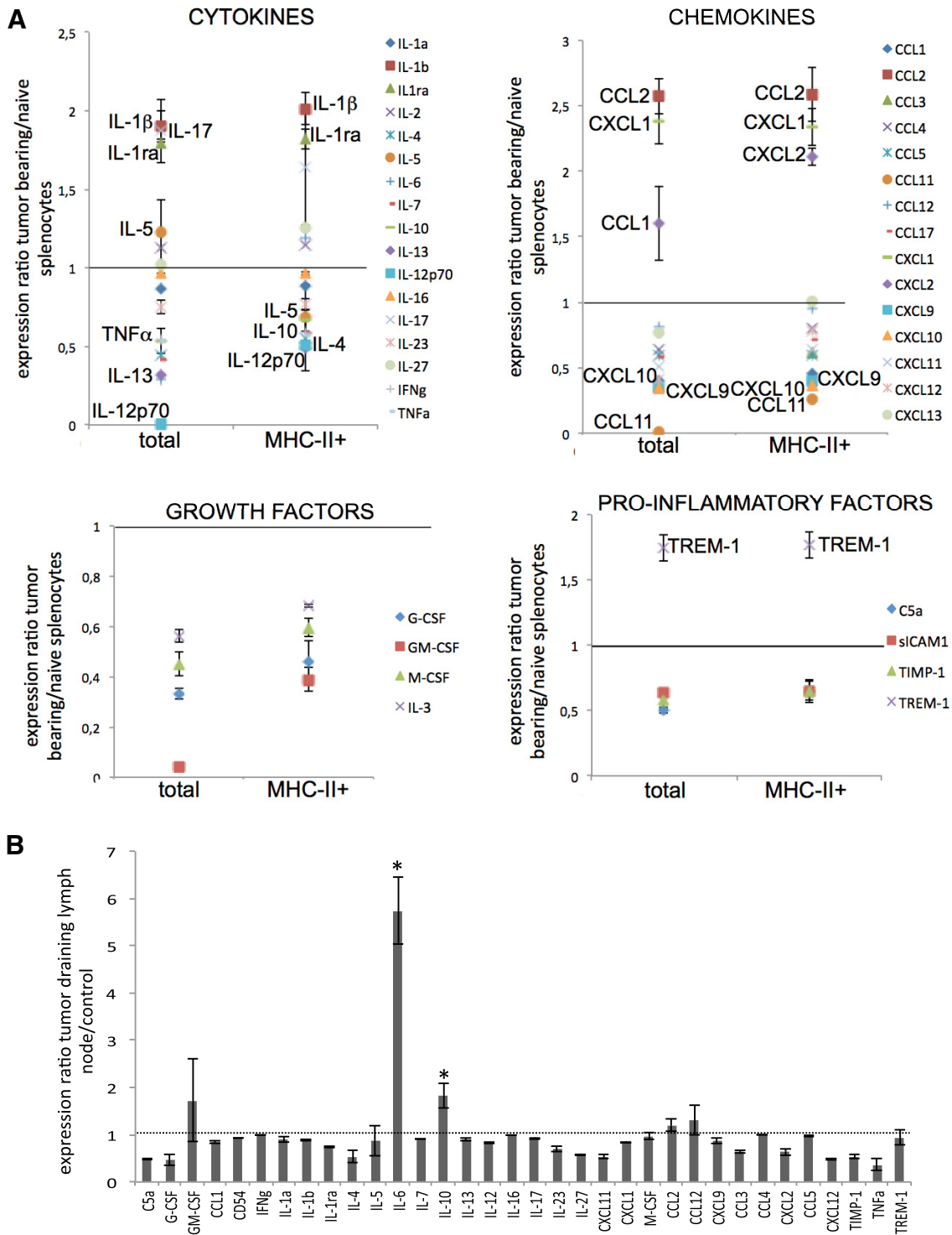
Figure 5. Cytokine-expression profile in the spleen and lymph nodes of tumor-bearing mice. (A) Total nucleated spleen cell protein extracts (total) or MHC-II+-sorted splenocytes (MHC-II+) were prepared, according to the Cytokine Proteome Array kit (R&D Systems) instructions. The same amount of protein (50 μg) from each preparation was incubated with each membrane containing the immobilized antibodies. The results represent the ratio of cytokine expression between spleens from mice with tumors and naive mice. Results are the average of three independent experiments. Names of molecules within the graph area indicate significant variation of expression between naive and tumor. Black lines mark Expression Ratio 1. sICAM1, soluble ICAM-1; TIMP-1, tissue inhibitor of metalloproteinases-1. (B) The same experiment was performed using total cell suspension lysates from tumor-bearing mice draining lymph nodes or inguinal lymph nodes from naive mice. The expression ratio of each cytokine is depicted. *Significant differences between control and tumor-bearing mice.

Overall, except for the IL-17 expression, our results indicate the existence of a suppressive environment in the spleens of tumor-bearing mice.

Tumor draining lymph nodes may be another source of IL-10 and IL-6

To characterize better tumor effects on lymphoid tissues, we repeated the same experiment as described above but used the tumor draining lymph nodes and inguinal control lymph nodes from naive mice. As shown in Fig. 5B, IL-10 and mainly IL-6 were the only significantly up-regulated cytokines in tumor draining lymph nodes compared with lymph nodes of naive mice. One major concern with this experiment was the possibility of detection of molecules not expressed by lymph node cells but rather, drained from the tumor microenvironment. One argument against this possibility is the low expression ratio of CCL2 and detection of C5a, both of which displayed high expression or detection in the tumor microenvironment. Therefore, it seems that tumor draining lymph nodes were another source of IL-10 and IL-6. Interestingly, no inflammation or T cell activation-related cytokines were observed in these organs, again indicating that tumors could promote a suppressive environment in the host.

Suppressive environment in tumor-bearing hosts may be related to inefficiency of antigen presentation caused by IL-10

Our results indicate the possibility that TC-1 tumors may generate a suppressive environment in the host, inhibiting antitumor T cells. To test this hypothesis, we have transplanted naive T cells from C57BL/6 donors into $RAG1^{-/-}$ tumor-bearing recipients. Results in **Fig. 6A** show that homeostatic proliferation in $RAG1^{-/-}$ recipients generated 2.3-fold more T_{regs} in the lymph nodes of tumor-bearing mice than in controls.

Our group had shown previously that IL-10 was important for TC-1 tumor growth and tolerance toward tumor antigens, inducing T_{reg} responses [22]. To pursue this initial data and better understand IL-10 role in our model, we injected TC-1 tumor cells in $IL-10^{-/-}$ mice to evaluate tumor growth, cell signaling, and T cell activation. As expected, TC-1 tumor growth was inhibited in $IL-10^{-/-}$ mice (Fig. 6B). In the spleen, we did not observe differences in macrophage and monocyte populations' frequency between $IL-10^{-/-}$ and control WT mice (**Fig. 7A**). However, we observed an increase in the expression of antigen-presenting molecules, as shown in Fig. 7B and C. Within the $CD11b^+$ population, we observed an increased frequency of $CD80^+$ and $CD86^+$ cells, and within the F4/80 population, we observed an increase in $CD86^+$ cells (Fig. 7B). We also observed an increase in the frequency of $CD11b^+MHC-II^+$ cells in $IL-10^{-/-}$ mice (Fig. 7C). Finally, we observed that APCs from WT tumor-bearing mice could inhibit T cell proliferation induced by PHA, whereas APCs from $IL-10^{-/-}$ mice did not have this suppressive effect (Fig. 7D). Accordingly, to the increase in antigen-presenting accessory molecules, we observed that in $IL-10^{-/-}$ mice, there was an increase in the expression of phosphorylated NF-κB com-
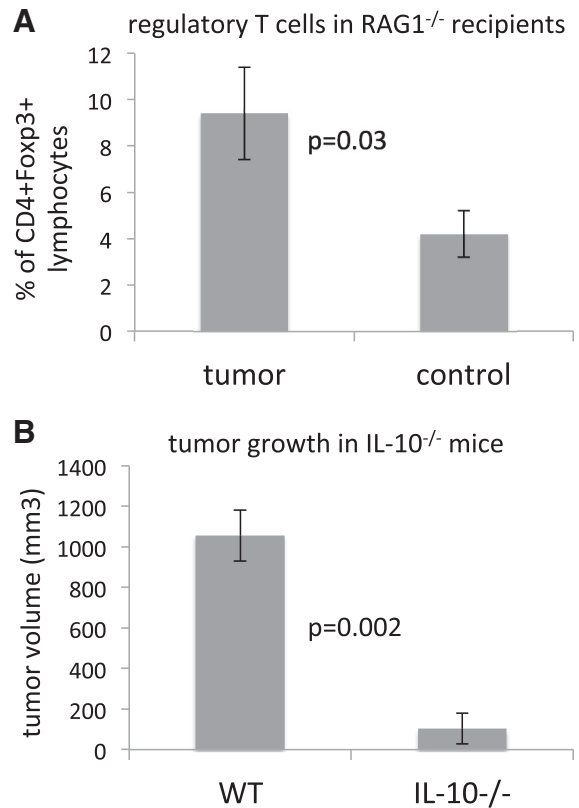

Figure 6. TC-1 tumors promote T_{reg} expansion, possibly through an IL-10-dependent mechanism. (A) T cells isolated from C57BL/6 naive mice were transplanted through the tail vein into $RAG1^{-/-}$ recipients, with or without TC-1 tumors. TC-1 tumors in $RAG1^{-/-}$ recipients displayed ~0.5-cm diameter at the moment of T cell transplant. A total of 2×10^6 lymphocytes was injected in each recipient. Fourteen days after transplant, mice were killed and peripheral lymph nodes harvested. Lymph node single-cell suspensions were stained with anti-CD4 and anti-CD25. Immediately after that, cells were fixed, permeabilized, and stained with anti-Foxp3 (eBioscience). Suspensions were analyzed in a FACSCalibur and differences between frequencies of the T_{reg} population evaluated by t-test (P<0.05). (B) TC-1 cells (10^5 cells/animal) were injected in $IL-10^{-/-}$ mice and control C57BL/6 mice (WT). Mice were observed every 3 days for tumor detection until tumors, from any group, reached 1–1.2-mm diameter in one axis. Results are the average tumor volume for four mice in each experimental group. In all cases, significance between experimental groups was determined by t-test.

pared with control mice in APCs from the spleen (Fig. 7E). These results segregate myeloid cell accumulation from phenotype modulation. IL-10 controls phenotype, but we still need to establish which factors control cell accumulation.

DISCUSSION

Tumors are complex structures containing different types of cells and molecules that influence neighbor cells as well as other tissues. It is well known that in cancer patients, T_{regs}, macrophages, and myeloid-derived cells play a role in tolerance toward tumor antigens [4–6]. Our laboratory has been
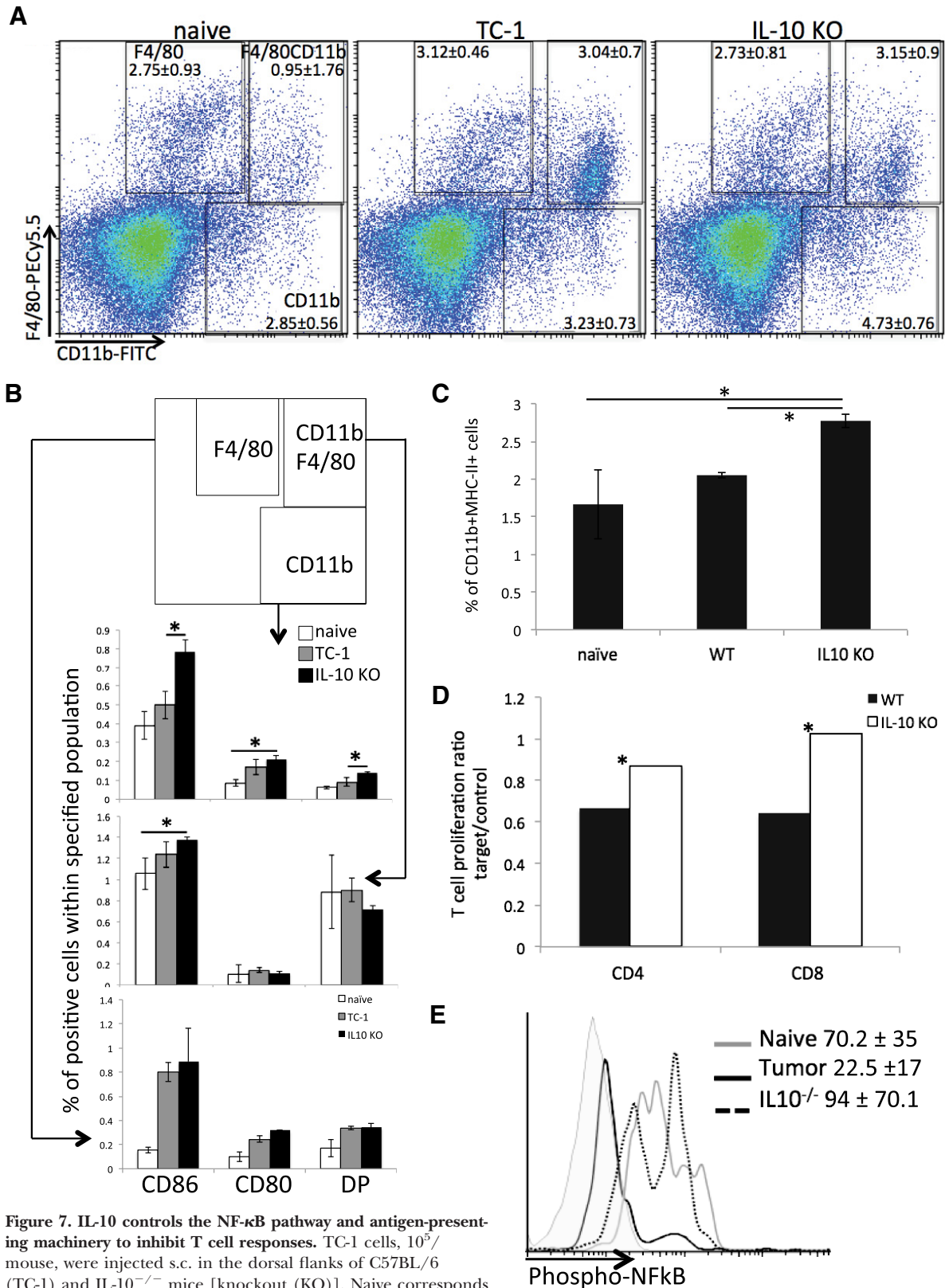
Figure 7. IL-10 controls the NF-κB pathway and antigen-presenting machinery to inhibit T cell responses. TC-1 cells, $10^5/$ mouse, were injected s.c. in the dorsal flanks of C57BL/6 (TC-1) and IL-10$^{-/-}$ mice [knockout (KO)]. Naive corresponds to mice that were not injected. When tumors in the TC-1 group reached 1–1.2 mm in diameter, we killed the mice and harvested the spleens. Nucleated splenocytes were prepared and incubated with antibodies against the indicated surface markers (A and B). Cells were analyzed by flow cytometry in a FACSCanto, where 50,000 events were acquired/sample. (A and B) Same batch of cells, where analyses of CD80 and CD86 frequency are measured within each population gate, as indicated in

interested in evaluating the tumor microenvironment effect on the host's immune system, mainly regarding leukocyte homeostasis and antigen-presentation potential, which obviously directly determines adaptive immune responses. Leukocytosis is an increase in the leukocyte cell numbers in an organism. It has been observed in patients with solid tumors. Its etiology may be iatrogenic (cytokine-based therapy), infectious (lymphocytic leukocytosis), or triggered by signals generated in the tumor microenvironment, as GM-CSF, G-CSF and IL-3 [7, 33, 34]. Patients with cervical cancer may develop leukocytosis, which is a poor prognostic factor for patients with recurrent disease [19, 35–37]. We have shown previously that HPV-positive cervical cancer-derived cell lines induced leukocytosis in immunodeficient mice, whereas a HPV-negative cervical cancer-derived cell failed to do so [23]. Interestingly, the in vivo cytokine-expression profile of the HPV-positive cell lines was similar among them but different from the prolife observed in the HPV-negative cell line [23]. In the current work, we show data regarding the TC-1 HPV16 tumor model, which was generated from C57BL/6 lung keratinocytes, therefore allowing us the benefit to study a model with adaptive immune responses. We observed accumulation of myeloid cells in the host's lymphoid organs. We were somewhat surprised by the small increase in cell proliferation in bone marrow cell populations of tumor-bearing mice compared with naive animals. We believe that this might reflect cell accumulation as a result of longer cell half-life or lack of cell emigration from the marrow. We believe the last possibility is rather unlikely as a result of the high expression of chemokines in spleen and tumor. However, we have not yet characterized chemokine receptor expression or cell half-life in the bone marrow. On the other hand, we observed the activation of tyrosine receptors Tie-2, Axl, Dtk, and EphA7, indicating that processes, such as angiogenesis, erythropoiesis, and cell differentiation, in the bone marrow could be modulated by tumors. Moreover, evidence of increased production of Tie-2 in patients with cervical cancer has been described previously in the literature [38]. In the spleen, we observed that myeloid cell accumulation was accompanied by a significant increase in cell proliferation. One of the cytokines expressed by TC-1 tumor cells and other HPV16-associated tumors or tumor cell lines is IL-6 [23, 39]. Indeed, we observed that tumor cells, tumor-inflammatory infiltrate, and spleen myeloid APCs (CD19$^-$MHC-II$^+$) displayed constitu-

tive JAK2/STAT3 and STAT5 activation, which could be, at least in part, responsible for myeloid cell proliferation and also for IL-10 expression by tumor-infiltrating macrophages [40, 41]. Other cytokines may also play a role in this process, such as G-CSF and IL-3, both expressed by tumor cells. Contrary to the activation of the IL-6/STAT axis, we observed down-regulation of NF-κB phosphorylation on serine 536 in tumor macrophages and spleen myeloid APCs. Phosphorylation of serine 536 is an early event in NF-κB activation, necessary for acetylation and full transcription activation [42, 43]. Accordingly, to this data, we observed down-regulation of IL-12 expression in the spleen of tumor-bearing mice [44], which together with low basal costimulatory molecule expression and positive IL-10 expression, suggests a suppressive environment in the host. The fact that homeostatic T cell proliferation generated a twofold increase in the number of T$_{regs}$ in tumor-bearing recipients than in naive RAG1$^{-/-}$ recipients reinforces the hypothesis. Again, we show that IL-10 is a key molecule in the orchestration of host tolerance toward tumor antigens. In fact, IL-10 promoter polymorphism -819C/T, which leads to higher IL-10 expression [45], represents an increased risk to cervical cancer development [46]. Concerning cervical cancer, most research groups obtained results that indicate that IL-10 plays a role in suppression of anti-HPV responses, therefore, facilitating tumor growth [47]. Indeed, our data show that IL-10 is one of the factors inhibiting NF-κB, although based on our experiments, we could not identify the exact molecular mechanism underlying this inhibition. However, our results show that the accumulation of suppressor myeloid cells triggered by the tumor is a multifactorial effect, where IL-10 plays a role in determining the cells' phenotype but does not affect cell proliferation or accumulation.

The phenotype of the cells that accumulate in the bone marrow and spleen of tumor-bearing mice was CD11b$^+$Gr1^{low}. However, in the tumors, we found that the majority of infiltrating cells was macrophages. We have dissected the cytokine-expression profile in the tumor microenvironment as well and observed that tumor cells expressed growth factors, myeloid cell-attracting chemokines, and IL-6. TAM expressed receptors to chemokines, myeloid cell-attracting chemokines, IL-10 and IL-5, as well as receptors for IL-10, IL-1, IL-6, and TNF-α, displaying a mixed phenotype regarding inflammation. Finally, the myeloid cell population CD11b$^+$Gr1$^+$ expressed proin-

---

the schemes above each histogram. (B) Diagram corresponding to gates within which CD80 and CD86 expression is identified on the top, with arrows pointing to analysis of each represented population. DP, CD80/CD86 double-positive. (C) Cells from the same suspensions were stained with anti-CD11b and anti-MHC-II and analyzed by flow cytometry. In all cases, differences between experimental groups were tested by one-way ANOVA and *t*-test between each pair of experimental groups. *Differences between pairs tested by *t*-test, where $P < 0.05$. (D) T cell suppression assay. Lymph node single-cell suspensions from naive donors were labeled with cell trace and incubated with PHA. To these cultures, we added CD11b$^+$ splenocytes sorted from C57/BL (WT) or IL-10$^{-/-}$ tumor-bearing mice. Five days later, cells were harvested, labeled with anti-CD4 and anti-CD8, and analyzed by flow cytometry. Data are represented as the ratio of the percent of CellTrace dim T cells in PHA-treated and control (nonstimulated) cultures. *Difference in T cell proliferation ratio in WT and IL-10$^{-/-}$ was significant, tested by *t*-test, $P < 0.05$. (E) Splenocytes from C57BL/6 (tumor) or IL-10$^{-/-}$ tumor-bearing or naive mice were labeled with anti-CD19 and anti-MHC-II. Cells were then fixed, permeabilized, and incubated with anti-phospho-NF-κB and analyzed by flow cytometry. Histograms represent the phospho-NF-κB of the CD19$^-$MHC-II$^+$ population in a representative sample. Average of MFI values in each experimental group is shown on the right. The gray, shaded histogram corresponds to cells incubated only with secondary antibody. The difference in the expression of phospho-NF-κB in IL-10 and C57BL/6 tumor-bearing mice was statistically significant, tested by *t*-test ($P=0.02$).

flammatory molecules. The expression profile of this population could indicate this is a bona fide inflammatory population. However, TREM-1, typically expressed by neutrophils, is also known to be expressed by MDSC [48]. Interestingly, although in a very different background and from a very different origin, in SiHa tumors (HPV16-positive), the leukocyte infiltrate displayed a remarkably similar cytokine profile as TAM from TC-1 tumors. This suggests that HPV16 tumors modulate leukocytes in a similar way, independently of the cell origin. Moreover, data from the literature have shown that supernatant from HPV-positive tumor cell lines secretes IL-6 and PGE2, inducing a suppressor phenotype in in vitro-differentiated dendritic cells, which in turn, express IL-10 instead of IL-12 [39]. These results are similar to those observed in our model.

Although we do not know which cells migrate to the tumor to differentiate into macrophages, we observed common signaling signatures between TAM and myeloid cells in the spleen. This included NF-κB down-regulation, JAK/STAT activation, and Akt constitutive activation, which could cooperate in inducing cell proliferation. Another common feature was CCL2 expression. CCR2, the receptor for CCL2 and other chemokines, was described previously as responsible for the recruitment of macrophages to HPV-associated lesions in a mouse transgenic model [49]. Interestingly, IL-10 can induce CCL2 expression [50]. In the tumor, inflammatory-infiltrating populations expressed more CCL2 than the TC-1 tumor cells, which may be an effect of autocrine signaling by IL-10, as the CD45$^+$ cells in the tumor expressed both IL-10R chains. As far as we were able to characterize, the only sources of IL-10 in mice with TC-1 tumors were TAM and to a lesser extent, the tumor draining lymph node. As this cytokine affected cells in the spleen, our observation underscores the systemic effects that tumors can have on cells in other tissues.

Some of the chemokines expressed in the tumor environment, including ligands for CXCR3, target T lymphocytes, which are not recruited to these tumors. It is possible that the lack of T cell activation in secondary lymphoid organs is responsible for the lack of T cells infiltrating the tumor. We have reported previously that depletion of TAM and reduction of myeloid cells to normal numbers in the spleen, allow expansion and infiltration of anti-HPV CD8 T cells, resulting in inhibition of tumor growth [21]. Interestingly, Choyce and collaborators [51] have shown, using a keratin 14/HPV16 E7 (K14E7) transgenic model, that T cells infiltrate hyperplasic premalignant skin and inhibit anti-tumor T cell responses. Although apparently different, we observe the association of suppressor T cells with tumor growth, in spite of important differences in the experimental models. Our work is focused on antigen presentation by myeloid cells, and we believe it would be very interesting to evaluate the phenotype of APCs this model.

To the best of our knowledge, there are no other studies exploring systemic effects of HPV16-associated tumors to the same extent of the present report. Our results are important and should be considered in the following situations: (1) infusion of T cells after chemo- or radiotherapy, where cells will proliferate in the host and will be subjected to the suppressor environment in the organism; (2) specifically regarding HPV

infections; considering that a significant percentage of anogenital and oropharyngeal tumors is also associated to HPV infection, it should be explored if similar events occur in these tumors and implement strategies to overcome them to obtain more efficient therapies; (3) is it possible to control leukocytosis, and will these patients have better survival rates? We believe that the answer to the last question will require a combination of agents to block factors that lead to myeloid cell proliferation and recruitment, creating a time window where T cell or dendritic cell-based therapies may be efficient in triggering anti-tumor immune responses.

AUTHORSHIP

S.C.S. performed, with help from R.A.M.R., protein-expression experiments, except for the cytokine proteome array, and helped with the studies of cell signaling through flow cytometry and BrdU incorporation assays. A.B. did the mRNA expression-prolife analysis. E.B. and P.S.A.S. reviewed data and this manuscript. A.P.L. wrote this manuscript, coordinated this study, and performed all other experiments.

ACKNOWLEDGMENTS

REFERENCES

1. Hanahan, D., Weinberg, R. A. (2011) Hallmarks of cancer: the next generation. *Cell* **144,** 646–674.
2. Guerra, C., Collado, M., Navas, C., Schuhmacher. A. J., Hernández-Porras, I., Cañamero, M., Rodriguez-Justo, M., Serrano, M., Barbacid, M. (2011) Pancreatitis-induced inflammation contributes to pancreatic cancer by inhibiting oncogene-induced senescence. *Cancer Cell* **19,** 728–739.
3. Barashi, N., Weiss, I. D., Wald, O., Wald, H., Beider, K., Abraham, M., Klein, S., Goldenberg, D., Axelrod, J., Pikarsky, E., Abramovitch, R., Zeira, E., Galun, E., Peled, A. (2013) Inflammation induced hepatocellular carcinoma is dependent on CCR5. *Hepatology* **58,** 1021–1030.
4. Sevko, A., Umansky, V. (2013) Myeloid-derived suppressor cells interact with tumors in terms of myelopoiesis, tumorigenesis and immunosuppression, thick as thieves. *J. Cancer* **4,** 3–11.
5. Baay, M., Brouwer, A., Pauwels, P., Peeters, M., Lardon, F. (2011) Tumor cells and tumor-associated macrophages, secreted proteins as potential targets for therapy. *Clin. Dev. Immunol.* **2011,** 1–12.
6. Tanchot, C., Terme, M., Pere, H., Tran, T., Benhamouda, N., Strioga, M., Banissi, C., Galluzzi, L., Kroemer, G., Tartour, E. (2012) Tumor-infiltrating regulatory T cells, phenotype, role, mechanism of expansion in situ and clinical significance. *Cancer Microenviron.* **6,** 147–157.
7. Wilcox, R. (2010) Cancer-associated myeloproliferation, old association, new therapeutic target. *Mayo Clin. Proc.* **85,** 656–663.
8. Kusmartsev, S., Gabrilovich, D. I. (2002) Immature myeloid cells and cancer-associated immune suppression. *Cancer Immunol. Immunother.* **51,** 293–298.
9. Neuhauser, C. (2009, July 27) Cancer cell kinetics. *Cancer Tumor Kinetics,* from http://bioquest.org/oakwood2008/wp-content/blogs.dir/files/2009/07/cancertumorkinetics.pdf.

10. Walboomers, J. M., Jacobs, M. V., Manos, M. M., Bosch, F. X., Kummer, J. A., Shah, K. V., Snijders, P. J., Peto, J., Meijer, C. J., Muñoz, N. (1999) Human papillomavirus is a necessary cause of invasive cervical cancer worldwide. *J. Pathol.* **189,** 12–19.

11. Moscicki, A. B., Schiffman, M., Burchell, A., Albero, G., Giuliano, A. R., Goodman, M. T., Kjaer, S. K., Palefsky, J. (2012) Updating the natural history of human papillomavirus and anogenital cancers. *Vaccine* **30** (Suppl. 5), F24–F33.

12. Gillison, M. L., Alemany, L., Snijders, P. J., Chaturvedi, A., Steinberg, B. M., Schwartz, S., Castellsagué, X. (2012) Human papillomavirus and diseases of the upper airway, head and neck cancer and respiratory papillomatosis. *Vaccine* **30** (Suppl. 5), F34–F54.

13. Hammes, L. S., Tekmal, R. R., Naud, P., Edelweiss, M. I., Kirma, N., Valente, P. T., Syrjänen, K. J., Cunha-Filho, J. S. (2007) Macrophages, inflammation and risk of cervical intraepithelial neoplasia (CIN) progression—clinicopathological correlation. *Gynecol. Oncol.* **105,** 157–165.

14. Mazibrada, J, Rittà, M., Mondini, M., De Andrea, M., Azzimonti, B., Borgogna, C., Ciotti, M., Orlando, A., Surico, N., Chiusa, L., Landolfo, S., Gariglio, M. (2008) Interaction between inflammation and angiogenesis during different stages of cervical carcinogenesis. *Gynecol. Oncol.* **108,** 112–120.

15. Kobayashi, A., Weinberg, V., Darragh, T., Smith-McCune, K. (2008) Evolving immunosuppressive microenvironment during human cervical carcinogenesis. *Mucosal Immunol.* **1,** 412–420.

16. Woo, Y. L., Sterling, J., Damay, I., Coleman, N., Crawford, R., van der Burg, S. H., Stanley, M. (2008) Characterising the local immune responses in cervical intraepithelial neoplasia, a cross-sectional and longitudinal analysis. *BJOG* **115,** 1616–1621.

17. Piersma, S. J., Jordanova, E. S., van Poelgeest, M. I., Kwappenberg, K. M., van der Hulst, J. M., Drijfhout, J. W., Melief, C. J., Kenter, G. G., Fleuren, G. J., Offringa, R., van der Burg, S. H. (2007) High number of intraepithelial CD8+ tumor-infiltrating lymphocytes is associated with the absence of lymph node metastases in patients with large early-stage cervical cancer. *Cancer Res.* **67,** 354–361.

18. Welters, M. J., van der Logt, P., van den Eeden, S. J., Kwappenberg, K. M., Drijfhout, J. W., Fleuren, G. J., Kenter, G. G., Melief, C. J., van der Burg, S. H., Offringa, R. (2006) Detection of human papillomavirus type 18 E6 and E7-specific CD4+ T-helper 1 immunity in relation to health versus disease. *Int. J. Cancer* **118,** 950–956.

19. Mabuchi, S., Matsumoto, Y., Hamasaki, T., Kawano, M., Hisamatsu, T., Mutch, D. G., Kimura, T. (2012) Elevated white blood cell count at the time of recurrence diagnosis is an indicator of short survival in patients with recurrent cervical cancer. *Int. J. Gynecol. Cancer* **22,** 1545–1551.

20. Lin, K. Y., Guarnieri, F. G., Staveley-O'Carroll, K. F., Levitsky, H. I., August, J. T., Pardoll, D. M., Wu, T. C. (1996) Treatment of established tumors with a novel vaccine that enhances major histocompatibility class II presentation of tumor antigen. *Cancer Res.* **56,** 21–26.

21. Lepique, A. P., Daghastanli, K. R., Cuccovia, I. M., Villa, L. L. (2009) HPV16 tumor associated macrophages suppress antitumor T cell responses. *Clin. Cancer Res.* **15,** 4391–4400.

22. Bolpetti, A., Silva, J. S., Villa, L. L., Lepique, A. P. (2010) Interleukin-10 production by tumor infiltrating macrophages plays a role in human papillomavirus 16 tumor growth. *BMC Immunol.* **7,** 11–27.

23. Stone, S. C., Rossetti, R. A. M., Lima, A. M., Lepique, A. P. (2014) HPV associated tumor cells control tumor microenvironment and leukocytosis in experimental models. *Immunity, Inflammation and Disease,* John Wiley & Sons, Hoboken, NJ, USA, http://onlinelibrary.wiley.com/doi/10.1002/iid3.21/full.

24. Friedl, F., Kimura, I., Osato, T., Ito, Y. (1970) Studies in a new human cell line (SiHa) derived from carcinoma of uterus. I. Its establishment and morphology. *Proctol. Soc. Exp. Biol. Med.* **135,** 543–545.

25. Montag, D. T., Lotze, M. T. (2006) Rapid flow cytometric measurement of cytokine-induced phosphorylation pathways [CIPP] in human peripheral blood leukocytes. *Clin. Immunol.* **121,** 215–226.

26. Gabrilovich, D. I., Velders, M. P., Sotomayor, E. M., Kast, W. M. (2001) Mechanism of immune dysfunction in cancer mediated by immature Gr-1+ myeloid cells. *J. Immunol.* **166,** 5398–5406.

27. Van Ginderachter J. A., Meerschaut, S., Liu, Y., Brys, L., De Groeve, K., Ghassabeh, G. H., Raes, G., De Baetselier, P. (2006) Peroxisome proliferator-activated receptor γ (PPARγ) ligands reverse CTL suppression by alternatively activated (M2) macrophages in cancer. *Blood* **108,** 525–535.

28. Zitvogel, L., Kepp, O., Galluzzi, L., Kroemer, G. (2012) Inflammasomes in carcinogenesis and anticancer immune responses. *Nat. Immunol.* **13,** 343–351.

29. Li, Y., de Haar, C., Chen, M., Deuring, J., Gerrits, M. M., Smits, R., Xia, B., Kuipers, E. J., van der Woude, C. J. (2010) Disease-related expression of the IL6/STAT3/SOCS3 signaling pathway in ulcerative colitis and ulcerative colitis-related carcinogenesis. *Gut* **59,** 227–235.

30. Donkor, M. K., Sarkar, A., Savage, P. A., Franklin, R. A., Johnson, L. K., Jungbluth, A. A., Allison, J. P., Li, M. O. (2011) T cell surveillance of oncogene-induced prostate cancer is impeded by T cell-derived TGF-β1 cytokine. *Immunity* **35,** 123–134.

31. Dinarello, C. A. (1996) Biologic basis for interleukin-1 in disease. *Blood* **87,** 2095–2147.

32. Lawrence, T. (2009) The nuclear factor NF-κB pathway in inflammation. *Cold Spring Harb. Perspect. Biol.* **1,** a001651.

33. Kasuga, I., Makino, S., Kiyokawa, H., Katoh, H., Ebihara, Y., Ohyashiki, K. (2001) Tumor-related leukocytosis is linked with poor prognosis in patients with lung carcinoma. *Cancer* **92,** 2399–2405.

34. Granger, J. M., Kontoyiannis, D. P. (2009) Etiology and outcome of extreme leukocytosis in 758 nonhematologic cancer patients, a retrospective, single-institution study. *Cancer* **115,** 3919–3923.

35. Nasu, K., Inoue, C., Takai, N., Kashima, K., Miyakawa, I. (2004) Squamous cell carcinoma of the cervix producing granulocyte colony-stimulating factor. *Obstet. Gynecol.* **104,** 1086–1088.

36. Matsumoto, Y., Mabuchi, S., Muraji, M., Morii, E., Kimura, T. (2010) Squamous cell carcinoma of the uterine cervix producing granulocyte colony-stimulating factor, a report of 4 cases and a review of the literature. *Int. J. Gynecol. Cancer* **20,** 417–421.

37. Qiu, M. Z., Xu, R. H., Ruan, D. Y., Li, Z. H., Luo, H. Y., Teng, K. Y., Wang, Z. Q., Li, Y. H., Jiang, W. Q. (2010) Incidence of anemia, leukocytosis, and thrombocytosis in patients with solid tumors in China. *Tumour Biol.* **31,** 633–641.

38. Kopczyńska, E., Makarewicz, R., Biedka, M., Kaczmarczyk, A., Kardymowicz, H., Tyrakowski, T. (2009) Plasma concentration of angiopoietin-1, angiopoietin-2 and Tie-2 in cervical cancer *Eur. J. Gynaecol. Oncol.* **30,** 646–649.

39. Heusinkveld, M., de Vos van Steenwijk, P. J., Goedemans, R., Ramwadhdoebe, T. H., Gorter, A., Welters, M. J., van Hall, T., van der Burg, S. H. (2011) M2 macrophages induced by prostaglandin E2 and IL-6 from cervical carcinoma are switched to activated M1 macrophages by CD4+ Th1 cells. *J. Immunol.* **187,** 1157–1165.

40. Finbloom, D. S., Winestock, K. D. (1995) IL-10 induces the tyrosine phosphorylation of tyk2 and Jak1 and the differential assembly of STAT1 α and STAT3 complexes in human T cells and monocytes. *J. Immunol.* **155,** 1079–1090.

41. Ding, Y., Chen, D., Tarcsafalvi, A., Su, R., Qin, L., Bromberg, J. S. (2003) Suppressor of cytokine signaling 1 inhibits IL-10-mediated immune responses. *J. Immunol.* **170,** 1383–1391.

42. Chaturvedi, M. M., Sung, B., Yadav, V. R., Kannappan, R., Aggarwal, B. B. (2011) NF-κB addiction and its role in cancer, 'one size does not fit all'. *Oncogene* **30,** 1615–1630.

43. Hoberg, J. E., Popko, A. E., Ramsey, C. S., Mayo, M. W. (2006) IκB kinase α-mediated derepression of SMRT potentiates acetylation of RelA/p65 by p300. *Mol. Cell. Biol.* **26,** 457–471.

44. Plevy, S. E., Gemberling, J. H., Hsu, S., Dorner, A. J., Smale, S. T. (1997) Multiple control elements mediate activation of the murine and human interleukin 12 p40 promoters, evidence of functional synergy between C/EBP and Rel proteins. *Mol. Cell. Biol.* **17,** 4572–4588.

45. Talaat, R. M., Abdel-Aziz, A. M., El-Maadawy, E. A., Abdel-Bary, N. (2014) Interleukin 10 gene promoter polymprphism and risk of diffuse large B cell lymphoma (DLBCL). *Egypt J. Med. Human Genet.* **15,** 7–13.

46. Yu, Z., Liu, Q., Huang, C., Wu, M., Li, G. (2013) The interleukin 10-819C/T polymorphism and cancer risk, a HuGE review and meta-analysis of 73 studies including 15,942 cases and 22,336 controls. *OMICS* **17,** 200–214.

47. Wang, Y., Liu, X., Li, Y., Li, O. (2013) The paradox of IL-10-mediated modulation in cervical cancer. *Biomed. Rep.* **1,** 347–351.

48. Zanzinger, K., Schellack, C., Nausch, N., Cerwenka, A. (2009) Regulation of triggering receptor expressed on myeloid cells 1 expression on mouse inflammatory monocytes. *Immunology* **128,** 185–195.

49. Pahler, J. C., Tazzyman, S., Erez, N., Chen, Y. Y., Murdoch, C., Nozawa, H., Lewis, C. E., Hanahan, D. (2008) Plasticity in tumor-promoting inflammation, impairment of macrophage recruitment evokes a compensatory neutrophil response. *Neoplasia* **10,** 329–340.

50. Sun, X. L., Louie, M. C., Vannella, K. M., Wilke, C. A., LeVine, A. M., Moore, B. B., Shanley, T. P. (2011) New concepts of IL-10-induced lung fibrosis, fibrocyte recruitment and M2 activation in a CCL2/CCR2 axis. *Am. J. Physiol. Lung Cell. Mol. Physiol.* **300,** L341–L353.

51. Choyce, A., Yong, M., Narayan, S., Mattarollo, S. R., Liem, A., Lambert, P. F., Frazer, I. H., Leggart, G. R. (2013) Expression of a single, viral oncoprotein in skin epithelium is sufficient to recruit lymphocytes. *PLoS One* **8,** e57798.